Published in final edited form as:
*Mol Immunol*. 2007 April ; 44(10): 2761–2771.

# Role of Apoptotic Signaling Pathways in Regulation of Inflammatory Responses to Ricin in Primary Murine Macrophages

**Veselina Korcheva**[1], **John Wong**[1], **Meghan Lindauer**[1], **David B. Jacoby**[2], **Mihail S. Iordanov**[1], and **Bruce Magun**[1,3]

***1****Department of Cell and Developmental Biology, Oregon Health and Science University, Portland, Oregon, USA*

***2****Division of Pulmonary and Critical Care Medicine, Oregon Health and Science University, Portland, Oregon, USA*

## Abstract

Because of its lethal effects, ease of preparation, and ability to be delivered by aerosolization, ricin has been developed as a lethal weapon by various terrorist groups. When introduced into the pulmonary system of rodents, ricin causes pathological changes in the lung that are known to occur in acute respiratory distress syndrome (ARDS). Early response cytokines such as TNF-α and IL-1 are known to play a critical role in the pathogenesis of ARDS. Ricin induces the release of these proinflammatory cytokines and the transcriptional activation of the genes that encode them *in vitro* and *in vivo*. Macrophages, considered to act as upstream regulators of inflammatory cascades, may play a central role in the pathogenesis and the development of ricin-induced ARDS because of their ability to make and secrete proinflammatory cytokines. Exposure of primary macrophages to ricin *in vitro* led to activation of stress-activated protein kinases, increased expression of proinflammatory mRNA transcripts, subsequent increase in the synthesis and secretion of TNF-alpha, and apoptotic cell death. Interestingly, macrophages required the engagement of the apoptotic cascade for the maximal synthesis and release of some proinflammatory mediators. This work identifies a cross talk between the apoptotic and inflammatory signaling pathways induced by ricin in primary macrophages.

### Keywords

MAP kinases; cell death; TNF-α

## INTRODUCTION

The toxin ricin is currently listed as a category B priority pathogen for study in the biodefense strategic plan of the United States National Institutes of Health based on ricin's broad availability, ease of production, high toxicity, and potential for use as an agent of bioterrorism. In a terrorist situation, ricin would be most effectively distributed to human populations by aerosolization. Although data on aerosol-mediated toxicity of ricin is lacking in humans, studies performed in rodents and non-human primates have shown that the introduction of ricin

[3]Correspondence: Bruce Magun, Oregon Health and Science University, 3181 SW Sam Jackson Park Road, L215, Portland, Oregon; phone 503 494 7811; fax 503 494 4253; email magunb@ohsu.edu.

into the pulmonary system leads to acute lung injury and acute respiratory distress syndrome (ARDS) [1]. When delivered to animals through aerosolization, ricin induces in an early massive migration of inflammatory cells (polymorphonuclear cells, lymphocytes, and macrophages) to the lungs and causes apoptosis of the alveolar macrophages [2]. Subsequent effects of ricin toxicity include apoptosis and necrosis of bronchiolar epithelial cells and type II pneumocytes, resulting in the development of ARDS. Because of the rapid effects of ricin on macrophages, and in view of the role that macrophages play in elaborating proinflammatory cytokines in ARDS and other inflammatory conditions [3], several studies have centered on the *in vivo* and *in vitro* effects of ricin on macrophages [2,4-6].

Ricin is a 64 kDa toxic heterodimeric protein, extracted from beans of the castor plant, that consists of a 32 kDa A-chain bonded by a disulfide linkage to a 32 kDa B-chain [7]. Ricin enters cells through binding of its B chain to galactosyl residues that are present on the surfaces of most cells [7]. In addition, macrophages express mannose receptors capable of binding mannosylated or fucosylated glycoproteins such as ricin A1 and A2 chains [8-11]. The ability of ricin to bind to both galactosyl residues and mannose receptors on macrophages may explain the high sensitivity that these cells demonstrate toward ricin. After its internalization through receptor-mediated endocytosis and further intracellular transport through the vesicular system, the A-chain of ricin enters the cytosol, where it depurinates a single adenine in the sarcin/ricin loop of 28S rRNA [12]. The depurination of this critical adenine prevents the binding of elongation factor-2, thereby blocking protein translation.

By producing a lesion in the sarcin/ricin loop of 28S rRNA, ricin also activates a kinase cascade that leads to the phosphorylation and activation of the stress-activated protein kinases, c-Jun-N-terminal kinase (JNK) and p38 MAPK [13], which are members of a larger family of mitogen-activated protein kinases (MAPK) that include extracellular signal-regulated kinase 1/2 (ERK1/2). Whereas activation of JNK and p38 MAPK has been tied to activation of proinflammatory pathways, activation of ERK1/2 is generally associated with pathways that control proliferation, differentiation, and cell cycle progression [14]. Previously we demonstrated in a murine macrophage cell line (RAW264.7) that, in addition to inhibiting protein synthesis, ricin simultaneously activated all three MAP kinase superfamily members (JNK, p38 MAPK, and ERK1/2) [5]. The application of specific inhibitors of each the latter MAP kinase family members demonstrated that in macrophages the activation of these kinases were required, individually or in concert, for the transcriptional activation of a broad variety of genes that encode inflammatory mediators. These mediators included cytokines, chemokines, transcription factors, and cell surface molecules [5].

Recent studies have also demonstrated that ricin is a potent inducer of apoptosis in cultured cells [15-19]. Although the mechanism of ricin-triggered apoptosis and its possible relationship to translational inhibition and MAPK activation is poorly understood, Higuchi et al [17] reported a significant decrease in the number of apoptotic RAW 264.7 cells after ricin treatment in the presence of the specific p38 MAPK inhibitor SB202190. Studies on the ability of ricin and other protein synthesis inhibitors to cause apoptosis in U937 cells suggested that the induction of apoptosis by protein synthesis inhibitors is not entirely due to pure protein synthesis inhibition [18]. Higuchi et al [17] suggested a possible relationship between ricin-triggered apoptosis and secretion of the proinflammatory cytokine TNF-α.

Although recent studies in a variety of cell lines have focused either on inflammatory responses or on apoptosis, studies that relate the potential cross talk between apoptotic and inflammatory signaling pathways are lacking. In this work, we demonstrate the existence of cross talk between pathways that signal inflammatory responses and apoptosis in primary bone marrow derived macrophages. To our knowledge, these studies are the first to address the dual roles of

ricin, i.e. gene activation and apoptosis, in primary macrophages. We consider the relevance of these findings to the potential actions of ricin as a terrorist agent and to the potential application of ricin as a therapeutic agent for ablating macrophages in chronic inflammatory diseases.

## MATERIALS AND METHODS

### Animals and Animal Procedures

C57BL/6J mice were purchased from The Jackson Laboratory, Bar Harbor, ME. Male mice, 8 to 10 weeks of age, were used throughout the experiments. Before experimental procedures, mice were anesthetized intraperitoneally with 80 mg/kg of ketamine and 10 mg/kg of xylazine. Twenty micrograms per 100g body weight ricin were delivered intratracheally [20] through a 22G cannula (BD Biosciences, San Diego, CA). Animals were anesthetized and sacrificed at times up to 48 hours. In obtaining bronchoalveolar lavage fluid, the rib cage of each mouse was opened through a midline incision and the trachea was cannulated with a 22G cannula. Bronchoalveolar lavage was performed by the instillation and withdrawal of 1 ml Phosphate Buffered Saline (PBS) into the cannula (three times total). Lavage fluid was centrifuged at 500 × g for 5 min and the supernatant was saved for analysis. The cellular component of the lavage fluid was resuspended in 500 μl 0.8 × PBS and further concentrated in a Cytospin™ centrifuge (Thermo Electron Corporation, Waltham, MA), affixed to microscope slides, and stained with Giemsa. All animal procedures were performed according to protocols that have been approved by the Institutional Animal Care and Use Committee at Oregon Health and Science University, Portland, Oregon.

### Isolation of Bone Marrow- Derived Macrophages

Bone marrow macrophages were prepared from C57BL/6J mice, essentially as described [21]. Marrow was flushed from femurs and tibias with PBS and cultured in alpha-Minimum Essential Medium (αMEM, Cellgro, Herndon, VA), supplied with 10% Fetal Bovine Serum (FBS, Cellgro, Herndon, VA), 50 μg/ml gentamicin, and 100 ng/ml recombinant mouse Colony Stimulating Factor 1 (CSF-1, R&D Systems, Minneapolis, MN) for 72 hrs. The bone marrow macrophages were plated into 3.5 and 6 cm tissue culture plates (Sarstedt, Newton, NC). The adherent cells were replated in 10% FBS-αMEM, in the presence of 100 ng/ml CSF-1 for an additional 24 hrs to achieve equal density of cells on the plates.

### Isolation of Alveolar Macrophages

Alveolar macrophages were obtained from pooled bronchoalveolar lavage fluid centrifuged at low speed (500 × g) for 5 minutes, at which time the cells were transferred in αMEM (containing 10% FBS and 50 μg/ml gentamicin) into 3.5 cm plastic bacterial culture dishes. Cells from lavage fluid of 3 mice were pooled into one 3.5 cm plate. Macrophages readily attached to the plates within 30 minutes.

### Reagents and Antibodies

Ricin was purchased from Vector Laboratories (Burlingame, CA). The pan-caspase inhibitor zVAD.fmk and the fluorogenic caspase-9 substrate (cat.#218765) were obtained from Calbiochem (La Jolla, CA). Fluorogenic caspase-8 substrate was purchased from BD Biosciences-Pharmingen (San Diego, CA). The mouse TNF-α enzyme-linked immunosorbent assay (ELISA) Ready-Set-Go was purchased from eBioscience (San Diego, CA). CXCL1 was measured in a LiquiChip Workstation (Qiagen, Valencia, CA), as described by the manufacturer, with reagents purchased from Linco Research (St. Charles, Missouri). Antibodies against phospho-p38 MAPK, phospho-JNK, phospho-ERK1/2, and caspase-3,

were obtained from Cell Signaling Technology (Beverly, MA); antibodies against p38 and MEK2 were purchased from Santa Cruz Biotechnology (Santa Cruz, CA); antibody against F4/80 was obtained from Serotec (Raleigh, NC).

### Measurement of Protein Synthesis

Bone marrow macrophages were grown in 12-well tissue culture dishes in 10% FBS-αMEM. Cells were serum deprived for 60 min before the treatment with ricin. Two and one half hours after the addition of ricin, cells were exposed to 2 μCi of [$^3$H]-leucine in 300 μl of serum-free αMEM for 30 minutes. The incorporation of leucine was terminated by the addition of 10% trichloroacetic acid. Cells were washed three times with 5% trichloroacetic acid, followed by 88% formic acid to solubilize the trichloroacetic acid-insoluble proteins, and the samples were counted in a scintillation counter.

### Immunoblot Analyses

Bone marrow macrophages cultured in 3.5 cm tissue culture plates and alveolar macrophages cultured in 3.5 cm plastic bacterial plates were lysed in 250 μl of 2 × sodium dodecyl sulfate-polyacrylamide gel elecrophoresis (SDS-PAGE) loading buffer and boiled at 95°C for 5 minutes. The lysates were separated via 10% or 13% SDS-PAGE, transferred to a polyvinylidene difluoride membrane (Millipore, Bedford, MA), and probed with the corresponding primary antibodies.

### Immunocytochemical Analysis

For detection of F4/80 antigen, macrophages were fixed with 4% paraformaldehyde solution for 20 minutes at 4°C and stained in accordance with the instructions provided with the primary antibody.

### Phagocytosis Assay

Cells were grown on glass cover slips (Fisher Scientific, USA) in 12-well tissue culture plates. Before experiments, cells were serum-deprived for 60 min in αMEM. Rhodamine-labeled latex particles (Spherotech, cat. #FP08582, Libertyville, IL), 0.7-0.9 μm diameter, were added to the cell cultures. Phagocytosis of the latex particles by macrophages was detected by confocal microscopy.

### Assay for Caspase-8 and Caspase-9 Activity

Bone marrow macrophages were cultured in 12-well dishes at a concentration of $1\times10^6$ cells per well. After treatments, cells were harvested with 1 × PBS and centrifuged at 500 × g for 5 min at 4°C. Cell pellets were resuspended in 200 μl lysis buffer containing 10 mM Tris-HCl, pH 7.5, 10 mM $NaH_2PO_4/NaHPO_4$, 130 mM NaCl, 10 mM $Na_4O_7P_2$, and 1% Triton X-100. The lysates were incubated for 15 minutes on ice prior to centrifugation at 12,000 × g for 10 min at 4°C. Supernatants were stored at −80°C until assayed. The protein concentration of the supernatants was determined by using the Bradford assay, Bio-Rad Laboratories (Hercules, CA). The lysates (100 μg) were assayed in caspase assay buffer (40 mM Hepes-KOH, pH 7.4, 20% glycerol, and 4 mM DTT) in the presence of 50 μM Ac-IETD-AFC (substrate for caspase-8) or Ac-LEHD-AFC (substrate for caspase-9) for 60 min at 37°C. Fluorescence emission in a spectrofluorophotometer was measured at 460 nm, with excitation at 390 nm. Caspase activity, at various time points after addition of ricin, $(C_{activity})^{t=x}$, was determined by subtracting the fluorescence intensity of each sample, in arbitrary units, from the fluorescence intensity of control standard that lacked cellular extract, where $x$ = time after addition of ricin. Percentage increase in caspase activity (in Figure 4, panel A) was determined as $[(C_{activity})^{t=x}/(C_{activity})^{t=0}] \times 100$.

### RNA Isolation

Cells were directly lysed in TRIzol reagent (Invitrogen Life Technologies, Carlsbad, CA) in accordance with the manufacturer's instructions. Isolated RNA was further digested with DNase (Invitrogen Life Technologies). The integrity of RNA was determined by the appearance of intact 28S and 18S rRNA bands when analyzed by electophoresis on 1% agarose gels.

### Real-Time RT-PCR

Two μg RNA were reverse-transcribed in the presence of SuperScript II and oligo-dT primers (Invitrogen Life Technologies). The amplification of the cDNA was performed on an ABI Prism 7900HT sequence detection system (Applied Biosystems, Foster City, CA) in the presence of SYBR Green PCR Master Mix (Applied Biosystems) and 20 μmol/L of the corresponding sense and anti-sense RT-PCR primers in a 40-cycle PCR. Each PCR cycle had the following amplification parameters: denaturation at 95°C for 15 seconds, annealing at 55° C for 30 seconds, and extension at 72°C for 30 seconds. Fold induction in gene expression was measured using absolute quantification of a standard curve in arbitrary units. In order to rule out the possibility that contaminating DNA could be contributing to RT-PCR results, we also included RT negative reactions and template negative reactions for each primer pair.

### Sense and Anti-Sense RT-PCR Primer Sequences

All primers, as published previously [5], were designed by using MacVector and Primer Express software programs, and were synthesized by Invitrogen Life Technologies.

### Statistical Analyses

Individual groups were compared by using paired t-test analysis. To estimate p values, all statistical analyses were interpreted in a two-tailed manner. P values of $<0.05$ were considered statistically significant.

## RESULTS

### Effects of intratracheally administered ricin on alveolar macrophages

Delivery of 20 μg ricin per 100 g body weight to mice by intratracheal instillation initiated a severe inflammatory process in the lungs, characterized by neutrophilia, hemorrhage, destruction of alveoli, and increased expression of inflammatory cytokines and chemokines within the lungs and in the general circulation (manuscript submitted). Examination of Cytospin preparations from bronchoalveolar lavage of ricin-instilled mice revealed a reduction by 90% in the number of macrophages; the reduction in macrophage numbers was evident by 12 hrs and continued for 48 hrs (Figure 1A). Fluid from saline-instilled control animals showed a modest decrease in macrophage numbers at 12 hrs, which returned to normal values by 48 hrs. In lavage fluid from ricin-treated animals, but not saline-instilled animals, polymorphonuclear cell numbers increased dramatically between 24 and 48 hrs (Figure 1B and 1F). Macrophages isolated from lavage fluid of ricin-instilled mice displayed morphological changes consistent with cells undergoing apoptosis 12 hrs after the administration of the toxin (Figure 1, compare panels C and D). Inasmuch as macrophages represent the primary source of TNF-α production in pulmonary tissues [3], we determined whether the ricin-mediated depletion of macrophages would result in a change in TNF-α content of lavage fluid. The lavage fluid from ricin-instilled mice displayed an initial increase in concentration of TNF-α, which subsequently declined to basal levels by 48 hrs (Figure 1G). The large increase in levels of TNF-α observed in lavage fluid from saline-instilled mice at 24 and 48 hrs (Figure 1G) probably resulted from the non-specific inflammatory effects of instilled saline. Notably, by 48 hrs the

level of TNF-α in lavage fluid of ricin-instilled mice was significantly lower than in saline-instilled mice.

Because lavage fluid from ricin-instilled mice displayed a dramatic increase in the number of neutrophils between 24 and 48 hrs (Figure 1B), we determined whether lavage fluid would also display increased levels CXCL1, a chemokine that possesses strong chemoattractant activity for neutrophils [22]. Figure 1H demonstrates that levels of CXCL1 protein in lavage fluid increased approximately 100 fold following instillation of ricin, with the majority of the increase occurring between 24 and 48 hrs.

## Effects of ricin on MAP kinase signaling in primary murine macrophages in vitro

In view of the effects of ricin in alveolar macrophages showed *in vivo*, and because of their ability to elaborate proinflammatory cytokines and contribute to the generation of inflammatory processes, we decided to further examine their role *in vitro* in mediating ricin-induced inflammation. For these experiments, we employed primary explants of both alveolar macrophages (AM) and bone marrow-derived macrophages (BMM). We selected AM because of their obvious relevance to the problem under investigation, although the small numbers of macrophages obtained severely limited the number and type of *in vitro* experiments that could be performed. We selected BMM because a larger number of macrophages could be obtained for experimentation. The purity of the macrophage cultures was verified by expression of F4/80 antigen and by the ability of the cells to phagocytose fluorescent particles (data not shown). These analyses indicated that macrophage purity was >99% for both AM and BMM.

Exposure of cells to ricin resulted in the activation of p38 MAPK and JNK in both AM and BMM (Figure 2). In contrast to p38 MAPK and JNK, whose phosphorylation was increased in response to ricin, the basal level of phosphorylated ERK1/2 was reduced following exposure of cells to ricin (Figure 2). As previously reported by us [5,13], a direct relationship was observed between the ability of ricin to inhibit protein synthesis and to activate p38 MAPK and JNK. When administered to BMM over a broad range of concentrations (1 to 10,000 ng/ml), ricin induced a dose-dependent decrease in the levels of protein synthesis (Figure 2, lower panel) that was contemporaneous with the phosphorylation of p38 MAPK and JNK.

## Ricin-mediated gene expression in primary murine macrophages

MAP kinases have been implicated in regulating the expression of proinflammatory cytokines and chemokines both by enhancing the transcriptional rates and by prolonging the lifetime of mRNAs that encode these molecules [23,24]. We applied real-time RT-PCR in AM and BMM to examine the effects of ricin on the expression profiles of mRNAs encoding proinflammatory genes. We analyzed a subset of proinflammatory genes whose expression is elevated by ricin [5]. The evaluated gene products included the proinflammatory cytokines TNF-α and IL-β, a chemokine (CXCL1/Gro-α), and transcription factors (c-Jun and ATF3). The results were expressed as fold induction, using glyceraldehyde phosphate dehydrogenase (GAPDH) as an invariant comparator. Both AM and BMM displayed substantial increases in ricin-induced mRNA levels in all of the evaluated genes 5 hrs after addition of ricin. For several genes, the degree of increased expression differed between AM and BMM (Figure 3A). The inclusion of ricin resulted in the release of TNF-α protein into the culture medium of treated BMM (Figure 3B). The elevated secretion of TNF-α by macrophages exposed to ricin may result from the stimulated release of pre-existing stores and/or from the *de novo* synthesis of protein. In view of the partial inhibition of protein synthesis in BMM by 10ng/ml ricin (Figure 2, lower panel), it is possible that the ricin-induced secretion of TNF-α resulted exclusively by release of pre-existing stores of TNF-α protein and not by translation of newly transcribed TNF-α mRNA. To test this possibility, we exposed BMM to 10ng/ml ricin for 6h, at which time both the

secreted and residual TNF-α protein were measured by ELISA. As expected, exposure of cells to ricin resulted in secretion of TNF-α protein; the residual intracellular TNF-α protein amounted to approximately 5% of total amount (Figure 3C). By contrast, unstimulated macrophages failed to release detectable TNF-α protein. The total amount of TNF-α (residual plus released) from unstimulated cells amounted to less than 15% of the TNF-α from ricin-treated cells ($p<0.01$; Figure 3C), demonstrating that exposure of cells to ricin resulted in substantial *de novo* synthesis of TNF-α protein. Taken together, the data in Figures 2 and 3 indicate that, in the presence of ricin, BMM responded by increasing the expression of several proinflammatory genes. In addition, the cells retained the ability to translate the ricin-induced TNF-α mRNA, despite the partial inhibition of protein translation.

Taking into consideration the requirement of a disproportionate number of animals in order to obtain sufficient numbers of AM to perform experiments, we chose to continue our analysis of macrophage responses exclusively in BMM.

## Ricin triggered activation of caspases in BMM

In view of the evidence that intratracheal instillation of ricin elicited apoptosis of pulmonary macrophages *in vivo*, we further investigated the identity of the initiator caspases activated *in vitro*. Exposure of BMM to ricin for 6 hrs resulted in a 42% activation of caspase-8 and a 264% activation of caspase-9 (Figure 4A). Concomitant with activation of caspases-8 and -9 were the ricin-mediated cleavage and processing of procaspase-3 (Figure 4B, lanes 3 and 7). Beginning at 6 hrs, ricin-treated cells progressively detached from the culture dishes and, when examined microscopically, displayed all the morphological characteristics (such as nuclear fragmentation) of cells undergoing apoptosis (not shown). Taken together, the data in Figures 3 and 4 indicate that exposure of macrophages to ricin resulted in the simultaneous engagement of apoptotic machinery and the increased expression of proinflammatory mRNAs, at least one of which, TNF-α, was efficiently translated.

## Effect of the pan-caspase inhibitor zVAD.fmk on ricin-mediated gene expression profile

In view of the simultaneous activation of apoptotic and transcriptional pathways by ricin, we explored the possibility that the ricin-mediated increase in expression of proinflammatory RNAs may be influenced by engagement of the apoptotic program. To test this possibility, BMM were exposed to ricin for 4 and 6 hrs in the presence or absence of zVAD.fmk (Figure 4B). The effectiveness of zVAD.fmk as a caspase-3 inhibitor was demonstrated by the ability of zVAD.fmk to block the autocatalytic processing of p20 and p19 intermediate fragments into the mature, p17, form of the enzyme [25] (compare lanes 3, 4, 7, and 8, Figure 4B). Additionally, zVAD.fmk suppressed both the detachment of ricin-treated cells and the appearance of morphological characteristics of apoptosis that occurred in these cells (data not shown). Inasmuch as BMM appeared to express undetectable levels of PARP (a substrate and frequently employed indicator of caspase-3 activity), we employed the immunodetection of MEK2 to assess the effect of zVAD.fmk on caspase activity. MEK1 and MEK2 have been previously shown to be cleaved during apoptosis in a caspase-dependent manner [26]. Indeed, pretreatment of cells with zVAD.fmk prevented the ricin-induced cleavage of MEK2 (Figure 4B, lanes 3, 4, 7, and 8), indicating complete inhibition of caspase activity. As shown in Figure 5, the inclusion of zVAD.fmk with ricin for 5 hrs inhibited the ricin-mediated increase in expression of mRNA encoding TNF-α by 50% and caused a significant ($p<0.05$), but marginal, decrease in expression of mRNA encoding c-Jun, IL-1α and IL-1β. Inclusion of zVAD.fmk did not alter the expression of RNA encoding ATF3 or two chemokines, CXCL1 and CCL2. Interestingly, the ricin-mediated expression of mRNA encoding c-Fos increased two-fold in the presence of zVAD.fmk. Taken together, Figures 4 and 5 suggest that the ricin-mediated

engagement of apoptosis differentially affected the expression profiles of mRNAs that encode the proinflammatory genes that were examined.

The ability of zVAD.fmk to suppress the ricin-mediated expression of TNF-α mRNA mediated by ricin (Figure 5) suggests that caspase activity in macrophages may be required for maximal expression of the mRNA that encodes TNF-α. We measured the secretion of TNF-α into the culture medium in the presence or absence of zVAD.fmk (Figure 6) to determine whether the apoptosis-induced increase in expression of TNF-α mRNA would result in the appearance of increased levels of TNF-α protein in the medium. The results clearly show that zVAD.fmk suppressed by 80% the release of TNF-α into the medium of ricin-treated BMM. Taken together, the data in Figures 5 and 6 demonstrate that increased expression of TNF-α mRNA induced by engagement of the apoptotic program in macrophages resulted in increased secretion of TNF-α protein.

## DISCUSSION

Although data on the aerosol toxicity of ricin is lacking in humans, studies performed in rodents and non-human primates have shown that introduction of ricin into the pulmonary system causes effects on lung pathology that are known to occur in ARDS [1,2] and that lead to death 36 to 48 hrs later [27]. The aerosol-mediated delivery of ricin to animals has been shown to result in a massive inflammatory response, characterized by increased inflammatory cell counts [28]. Recent studies have shown that TNF-α and IL-1β are present in increased amounts in the bronchoalveolar lavage fluid of patients with ARDS [29,30] and initiate a proinflammatory cascade that plays a central role in the pathogenesis of ARDS [3]. TNF-α is derived predominantly from activated macrophages by the transcriptional modulation of the TNF-α gene [31,32], and the cytokine acts on a variety of cells via cell membrane-bound receptors [33].

The present study demonstrates that the intratracheal administration of ricin to mice resulted in a dramatic decrease in AM numbers over 48 hrs and was accompanied by widespread apoptosis of these cells. Previous studies reported that the intravascular administration of ricin resulted in depletion of Kupffer cells of liver [6,34], although the mechanism of depletion of these macrophage derivatives was not characterized. By employing transmission electron microscopy, Brown et al [2] reported that, following intratracheal instillation of ricin in rats, alveolar macrophages underwent nuclear changes characteristic of apoptosis. In other studies, we demonstrate in histological sections of lung tissue that instilled ricin leads to the apoptosis of alveolar macrophages (manuscript submitted).

In the current study, we present quantitative evidence that intratracheal administration of ricin depletes alveolar macrophages. Instillation of ricin resulted in an initial increase in TNF-α in the lavage fluid, with a peak of TNF-α observed at 12h post-instillation (Figure 1G). This initial release of TNF-α was followed by a substantial decrease in TNF-α to at least 48h. The continuing decline in TNF-α protein (Figure 1G) and numbers of AM (Figure 1A) in the lavage fluid from 12h to 48h are consistent with the appearance of apoptotic macrophages in lavage fluid obtained 12h after instillation of ricin (Figure 1D). The results from *in vitro* experiments on BMM were consistent with the *in vivo* data, inasmuch as they demonstrated that ricin induced a 10 to 20-fold increase in levels of TNF-α mRNA (Figure 3B,C) and the ultimate apoptosis of these cells (Figure 4). The demonstration in BMM *in vitro* that ricin induced the accumulation of mRNA encoding TNF-α (Figure 5) and the *de novo* synthesis and ultimate secretion of TNF-α (Figure 3C) prior to apoptosis (Figure 4B) demonstrates that death of macrophages occurred subsequent to the activation by ricin of a productive proinflammatory synthetic program. The pro-apoptotic effects of ricin on macrophages *in vivo* may be beneficial

to the host by serving to limit the potential local tissue damage that may occur upon uncontrolled macrophage activation.

In view of the early involvement of AM in ricin-induced pulmonary responses, we examined the proinflammatory consequences of ricin exposure in primary macrophages *in vitro*. We previously demonstrated that, in addition to inhibiting translation, ricin simultaneously activates a kinase cascade by producing a lesion in the peptidyl transferase center of 28S rRNA [13]. The depurination of this specific adenine (A4256 in mice) leads, through an unidentified transduction apparatus, to the activation of upstream kinases that lead to the ultimate activation of JNK and p38 MAPK [13]. Activation of JNK and p38 MAPK by proinflammatory stimuli has been shown to occupy a central role in mediating inflammatory processes [24,35-37]. We demonstrate that the *in vitro* administration of ricin to AM and BMM resulted in the phosphorylation of both p38 MAPK and JNK. In AM and BMM, the activation of these kinases was accompanied by increased expression of mRNAs encoding proinflammatory proteins, including cytokines, chemokines, and transcription factors (Figures 2 and 3). The quantitative differences in ricin-mediated gene expression that we have observed between AM and BMM are likely to reflect the presence of different macrophage subpopulations, which have been identified even among pulmonary macrophages [38]. For example, the secretion of IL-1 and IL-6 in response to LPS has been shown to differ between pulmonary interstitital macrophages and AM [39]. The high constitutive activation of ERK that we detected in BMM, in contrast to AM, (Figure 2) is another indicator of the differences that exist between these two macrophage subtypes.

We previously reported that in RAW 264.7 cells, a transformed murine macrophage cell line, ricin induced the activation of ERK1/2 in addition to JNK and p38 MAPK [5]. Interestingly, ricin failed to activate ERK1/2 in both AM and BMM. In addition to its inability to activate ERK1/2, ricin also failed to activate MEK1/2, Raf-1, and Ras, upstream kinases that participate in the ERK cascade (data not shown). The mechanisms responsible for the ability of ricin to activate ERK1/2 in RAW 264.7 cells, but not in BMM or AM, are unknown but may relate to differences in signaling mechanisms that control the cell cycle of continuous cell lines such as RAW 264.7 cells.

We sought to determine whether a functional relationship exists between the proapoptotic and proinflammatory consequences of ricin in macrophages. A concentration of ricin that resulted in both the increased expression of proinflammatory mRNAs and secretion of TNF-α protein (100 ng/ml) resulted in engagement of an apoptotic cascade that included activation of both apical (caspase-8 and caspase-9) and effector (caspase-3) caspases (Figure 4). Importantly, the moribund macrophages were engaged in the elaboration of proinflammatory mRNAs, including RNA encoding CXCL1, a chemokine that plays a role in neutrophil chemotaxis [22]. In stained tissue sections of lung from ricin-instilled mice, we have detected the accumulation of neutrophils in perivascular and peribronchial regions 48 hrs after instillation (manuscript submitted). The correlation between neutrophilia and appearance of CXCL1 protein in lavage fluid of ricin-instilled mice (Figure 1), and the ricin-induced expression of CXCL1 mRNA in macrophages *in vitro* (Figure 5), suggests that ricin may mediate the migration of neutrophils into the lung by acting directly on pulmonary macrophages.

The inclusion of the pan-caspase inhibitor zVAD.fmk with ricin led to an unexpected reduction (>50%) in the accumulation of TNF-α mRNA and protein. These data demonstrate that the engagement of the apoptotic cascade in macrophages not only failed to reduce the accumulation of an important initiator cytokine, TNF-α, but instead augmented both its transcription and ultimate release into the cell milieu (Figures 5 and 6). The inability of zVAD.fmk to alter the expression of transcripts encoding the chemokines CXCL1 and CCL2 (Figure 5) may

contribute to the large increase in neutrophils in lavage fluid observed between 24 and 48hrs after instillation of ricin. The increased expression of mRNA encoding c-Fos in the presence of zVAD.fmk suggests that the engagement of the apoptotic program by ricin may serve to suppress the transcription of some inflammatory gene products that are mediated by c-Fos.

In previous studies we demonstrated that the p38 MAPK inhibitor SB203580 strongly inhibited the ricin-induced expression of a variety of proinflammatory mRNAs in RAW264.7 cells [5]. The downstream targets of p38 MAPK include kinases and transcription factors, some of which belong to the AP-1/ATF family. Many of these transcription factors have been shown to participate in the activation of proinflammatory genes [23]. Our data reveal a strong correlation between the ability of ricin to mediate the activation/phosphorylation of JNK and p38 MAPK (Figure 2) and to increase the expression of genes that encode the transcription factors c-Jun, c-Fos, and ATF3 in macrophages *in vitro* (Figure 3).

Elucidating the mechanisms of ricin-induced apoptotic death in monocyte/macrophages may have therapeutic implications for the control of inflammatory diseases. The selective elimination of monocyte/macrophages in patients with rheumatoid arthritis through apoptosis induced by ricin-conjugated CD64 (a receptor that is constitutively expressed by monocyte/macrophages lineage [40]) decreases local proinflammatory activity and inhibits cartilage degradation [41,42]. Selective activation of macrophage cell death may thus reveal a novel approach in the treatment of rheumatoid arthritis. The pro-apoptotic effects of ricin-CD64 immunotoxin have also been shown to target macrophages that participate in chronic cutaneous inflammation, resulting in the effective resolution of both histological and clinical symptoms [43]. Application of ricin immunotoxins may also find application for a variety of human cutaneous diseases, such as cutaneous graft-versus host disease, chronic contact dermatitis, atopic dermatitis, and psoriasis [44]. Further studies that define the cellular and molecular mechanisms by which ricin controls both proinflammatory and pro-apoptotic outcomes should aid in this effort.

This work highlights the early and potentially prominent role occupied by macrophages in orchestrating inflammatory responses to ricin. Elucidating the pathways regulated by ricin in macrophages should aid in the development of therapeutic agents that are effective in treating human populations that have been exposed to aerosolized ricin and, more generally, may contribute to understanding the role that macrophages play in the development of ARDS.

**ACKNOWLEDGEMENTS**

These studies were supported by grants DK066439 and AI1059335 from the National Institutes of Health.

We acknowledge the important technical contributions of Thanh-Hoai Dinh.

## REFERENCES

1. Greenfield RA, Brown BR, Hutchins JB, Iandolo JJ, Jackson R, Slater LN, Bronze MS. Microbiological, biological, and chemical weapons of warfare and terrorism. Am J Med Sci 2002;323:326–40. [PubMed: 12074487]
2. Brown RF, White DE. Ultrastructure of rat lung following inhalation of ricin aerosol. Int J Exp Pathol 1997;78:267–76. [PubMed: 9505938]
3. Bhatia M, Moochhala S. Role of inflammatory mediators in the pathophysiology of acute respiratory distress syndrome. J Pathol 2004;202:145–56. [PubMed: 14743496]
4. Taylor CM, Williams JM, Lote CJ, Howie AJ, Thewles A, Wood JA, Milford DV, Raafat F, Chant I, Rose PE. A laboratory model of toxin-induced hemolytic uremic syndrome. Kidney Int 1999;55:1367–74. [PubMed: 10201001]

5. Korcheva V, Wong J, Corless C, Iordanov M, Magun B. Administration of ricin induces a severe inflammatory response via nonredundant stimulation of ERK, JNK, and P38 MAPK and provides a mouse model of hemolytic uremic syndrome. Am J Pathol 2005;166:323–39. [PubMed: 15632024]
6. Zenilman ME, Fiani M, Stahl P, Brunt E, Flye MW. Use of ricin A-chain to selectively deplete Kupffer cells. J Surg Res 1988;45:82–9. [PubMed: 3392996]
7. Barbieri L, Battelli MG, Stirpe F. Ribosome-inactivating proteins from plants. Biochim Biophys Acta 1993;1154:237–82. [PubMed: 8280743]
8. Battelli MG, Musiani S, Monti B, Buonamici L, Sparapani M, Contestabile A, Stirpe F. Ricin toxicity to microglial and monocytic cells. Neurochem Int 2001;39:83–93. [PubMed: 11408086]
9. Frankel AE, Fu T, Burbage C, Tagge E, Harris B, Vesely J, Willingham MC. Lectin-deficient ricin toxin intoxicates cells bearing the D-mannose receptor. Carbohydr Res 1997;300:251–8. [PubMed: 9202409]
10. Riccobono F, Fiani ML. Mannose receptor dependent uptake of ricin A1 and A2 chains by macrophages. Carbohydr Res 1996;282:285–92. [PubMed: 8901091]
11. Simmons BM, Stahl PD, Russell JH. Mannose receptor-mediated uptake of ricin toxin and ricin A chain by macrophages. Multiple intracellular pathways for a chain translocation. J Biol Chem 1986;261:7912–20. [PubMed: 3711116]
12. Olsnes S, Kozlov JV. Ricin. Toxicon 2001;39:1723–8. [PubMed: 11595634]
13. Iordanov MS, Pribnow D, Magun JL, Dinh TH, Pearson JA, Chen SL, Magun BE. Ribotoxic stress response: activation of the stress-activated protein kinase JNK1 by inhibitors of the peptidyl transferase reaction and by sequence-specific RNA damage to the alpha-sarcin/ricin loop in the 28S rRNA. Mol Cell Biol 1997;17:3373–81. [PubMed: 9154836]
14. Yoon S, Seger R. The extracellular signal-regulated kinase: multiple substrates regulate diverse cellular functions. Growth Factors 2006;24:21–44. [PubMed: 16393692]
15. Gan YH, Peng SQ, Liu HY. Molecular mechanism of apoptosis induced by ricin in HeLa cells. Acta Pharmacol Sin 2000;21:243–8. [PubMed: 11324424]
16. Rao PV, Jayaraj R, Bhaskar AS, Kumar O, Bhattacharya R, Saxena P, Dash PK, Vijayaraghavan R. Mechanism of ricin-induced apoptosis in human cervical cancer cells. Biochem Pharmacol 2005;69:855–65. [PubMed: 15710362]
17. Higuchi S, Tamura T, Oda T. Cross-talk between the pathways leading to the induction of apoptosis and the secretion of tumor necrosis factor-alpha in ricin-treated RAW 264.7 cells. J Biochem (Tokyo) 2003;134:927–33. [PubMed: 14769883]
18. Kageyama A, Kusano I, Tamura T, Oda T, Muramatsu T. Comparison of the apoptosis-inducing abilities of various protein synthesis inhibitors in U937 cells. Biosci Biotechnol Biochem 2002;66:835–9. [PubMed: 12036057]
19. Khan T, Waring P. Macrophage adherence prevents apoptosis induced by ricin. Eur J Cell Biol 1993;62:406–14. [PubMed: 7925496]
20. Hastings RH, Summers-Torres D. Direct Laryngoscopy in Mice. Contemp Top Lab Anim Sci 1999;38:33–35. [PubMed: 12086445]
21. Warren MK, Vogel SN. Bone marrow-derived macrophages: development and regulation of differentiation markers by colony-stimulating factor and interferons. J Immunol 1985;134:982–9. [PubMed: 2578168]
22. Geiser T, Dewald B, Ehrengruber MU, Clark-Lewis I, Baggiolini M. The interleukin-8-related chemotactic cytokines GRO alpha, GRO beta, and GRO gamma activate human neutrophil and basophil leukocytes. J Biol Chem 1993;268:15419–24. [PubMed: 8340371]
23. Kyriakis JM, Avruch J. Mammalian mitogen-activated protein kinase signal transduction pathways activated by stress and inflammation. Physiol Rev 2001;81:807–69. [PubMed: 11274345]
24. Herlaar E, Brown Z. p38 MAPK signalling cascades in inflammatory disease. Mol Med Today 1999;5:439–47. [PubMed: 10498912]
25. Sun XM, MacFarlane M, Zhuang J, Wolf BB, Green DR, Cohen GM. Distinct caspase cascades are initiated in receptor-mediated and chemical-induced apoptosis. J Biol Chem 1999;274:5053–60. [PubMed: 9988752]

26. McGuire TF, Trump DL, Johnson CS. Vitamin D(3)-induced apoptosis of murine squamous cell carcinoma cells. Selective induction of caspase-dependent MEK cleavage and up-regulation of MEKK-1. J Biol Chem 2001;276:26365–73. [PubMed: 11331275]
27. Wilhelmsen CL, Pitt ML. Lesions of acute inhaled lethal ricin intoxication in rhesus monkeys. Vet Pathol 1996;33:296–302. [PubMed: 8740703]
28. Franz, DR.; Jaax, JK. Ricin Toxin. In: Sidell, FR.; Takfuji, ET.; Franz, DR., editors. Textbook of Military medicine Part 1. Warfare, Weaponry, and the Casualty: Medical Aspects of Chemical and biological Warfare. Department of the Army; United States of America, Washington: 1997. p. 631-642.office of the Surgeon General
29. Park WY, Goodman RB, Steinberg KP, Ruzinski JT, Radella F 2nd, Park DR, Pugin J, Skerrett SJ, Hudson LD, Martin TR. Cytokine balance in the lungs of patients with acute respiratory distress syndrome. Am J Respir Crit Care Med 2001;164:1896–903. [PubMed: 11734443]
30. Siler TM, Swierkosz JE, Hyers TM, Fowler AA, Webster RO. Immunoreactive interleukin-1 in bronchoalveolar lavage fluid of high-risk patients and patients with the adult respiratory distress syndrome. Exp Lung Res 1989;15:881–94. [PubMed: 2612445]
31. Falvo JV, Uglialoro AM, Brinkman BM, Merika M, Parekh BS, Tsai EY, King HC, Morielli AD, Peralta EG, Maniatis T, Thanos D, Goldfeld AE. Stimulus-specific assembly of enhancer complexes on the tumor necrosis factor alpha gene promoter. Mol Cell Biol 2000;20:2239–47. [PubMed: 10688670]
32. Tsai EY, Falvo JV, Tsytsykova AV, Barczak AK, Reimold AM, Glimcher LH, Fenton MJ, Gordon DC, Dunn IF, Goldfeld AE. A lipopolysaccharide-specific enhancer complex involving Ets, Elk-1, Sp1, and CREB binding protein and p300 is recruited to the tumor necrosis factor alpha promoter in vivo. Mol Cell Biol 2000;20:6084–94. [PubMed: 10913190]
33. Cohen J. The immunopathogenesis of sepsis. Nature 2002;420:885–91. [PubMed: 12490963]
34. Bingen A, Creppy EE, Gut JP, Dirheimer G, Kirn A. The Kupffer cell is the first target in ricin-induced hepatitis. J Submicrosc Cytol 1987;19:247–56. [PubMed: 3599122]
35. Lee JC, Kumar S, Griswold DE, Underwood DC, Votta BJ, Adams JL. Inhibition of p38 MAP kinase as a therapeutic strategy. Immunopharmacology 2000;47:185–201. [PubMed: 10878289]
36. Lee JC, Kassis S, Kumar S, Badger A, Adams JL. p38 mitogen-activated protein kinase inhibitors--mechanisms and therapeutic potentials. Pharmacol Ther 1999;82:389–97. [PubMed: 10454214]
37. Karin M, Gallagher E. From JNK to pay dirt: jun kinases, their biochemistry, physiology and clinical importance. IUBMB Life 2005;57:283–95. [PubMed: 16036612]
38. Chandler DB, Kennedy JI, Fulmer JD. Studies of membrane receptors, phagocytosis, and morphology of subpopulations of rat lung interstitial macrophages. Am Rev Respir Dis 1986;134:542–7. [PubMed: 3752710]
39. Franke-Ullmann G, Pfortner C, Walter P, Steinmuller C, Lohmann-Matthes ML, Kobzik L. Characterization of murine lung interstitial macrophages in comparison with alveolar macrophages in vitro. J Immunol 1996;157:3097–104. [PubMed: 8816420]
40. Deo YM, Graziano RF, Repp R, van de Winkel JG. Clinical significance of IgG Fc receptors and Fc gamma R-directed immunotherapies. Immunol Today 1997;18:127–35. [PubMed: 9078685]
41. van Roon JA, van Vuuren AJ, Wijngaarden S, Jacobs KM, Bijlsma JW, Lafeber FP, Thepen T, van de Winkel JG. Selective elimination of synovial inflammatory macrophages in rheumatoid arthritis by an Fcgamma receptor I-directed immunotoxin. Arthritis Rheum 2003;48:1229–38. [PubMed: 12746896]
42. van Vuuren AJ, van Roon JA, Walraven V, Stuij I, Harmsen MC, McLaughlin PM, van de Winkel JG, Thepen T. CD64-directed immunotoxin inhibits arthritis in a novel CD64 transgenic rat model. J Immunol 2006;176:5833–8. [PubMed: 16670289]
43. Thepen T, van Vuuren AJ, Kiekens RC, Damen CA, Vooijs WC, van De Winkel JG. Resolution of cutaneous inflammation after local elimination of macrophages. Nat Biotechnol 2000;18:48–51. [PubMed: 10625390]
44. McCormick TS, Stevens SR, Kang K. Macrophages and cutaneous inflammation. Nat Biotechnol 2000;18:25–6. [PubMed: 10625384]

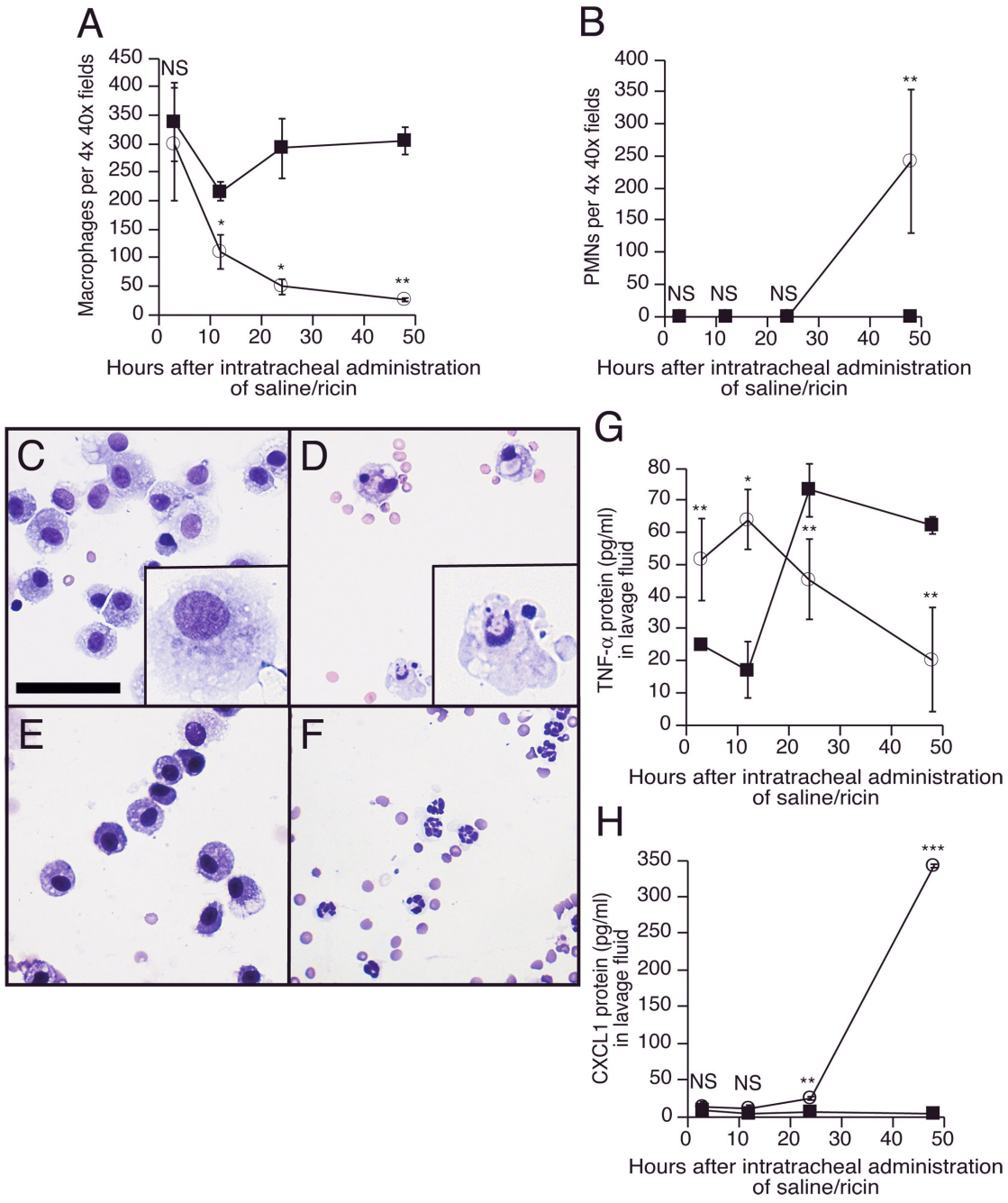


**Figure 1.**

A: Macrophage numbers in bronchoalveolar lavage fluid at designated times after intratracheal instillation of saline (filled squares) or 20 μg ricin /100 g bwt (open circles). B: Polymorphonuclear cell numbers (PMNs) in BAL at designated times after intratracheal instillation of saline (filled squares) or 20 μg ricin/100 g bwt (open circles). C-F: Cellular components from bronchoalveolar lavage, concentrated with Cytospin, and stained with Giemsa for leukocyte counting and assessment of cellular morphology. Scale bar equals 10 μm. In the lower right corner of panels C and D is a magnified image of a randomly selected cell from the corresponding field. C: Normal-appearing alveolar macrophages from lavage after intratracheal instillation of saline for 12 hrs. D: Apoptotic alveolar macrophages from

lavage after intratracheal instillation of 20 μg ricin per 100 g bwt for 12 hrs. E: Normal-appearing alveolar macrophages from lavage after intratracheal instillation of saline for 48 hrs. F: Polymorphonuclear cells predominate in the lavage fluid after intratracheal instillation of 20 μg ricin per 100 g bwt for 48 hrs. G: TNF-α protein from lavage fluid, measured by ELISA at designated times after intratracheal instillation of saline (filled squares) or 20 μg ricin/100 g bwt (open circles). H: CXCL1 protein from lavage fluid, measured by Luminex assay at designated times after intratracheal instillation of saline (filled squares) or 20 μg ricin /100 g bwt (open circles). For panels G and H, analyses at each time point were performed on three saline-instilled and three ricin-instilled animals. Displayed data were confirmed in three different experiments and are presented as mean ± standard error of the mean. Asterisks show comparison between treatments and controls. NS, not significantly different; *, $p<0.05$; **, $p<0.01$; ***, $p<0.001$.

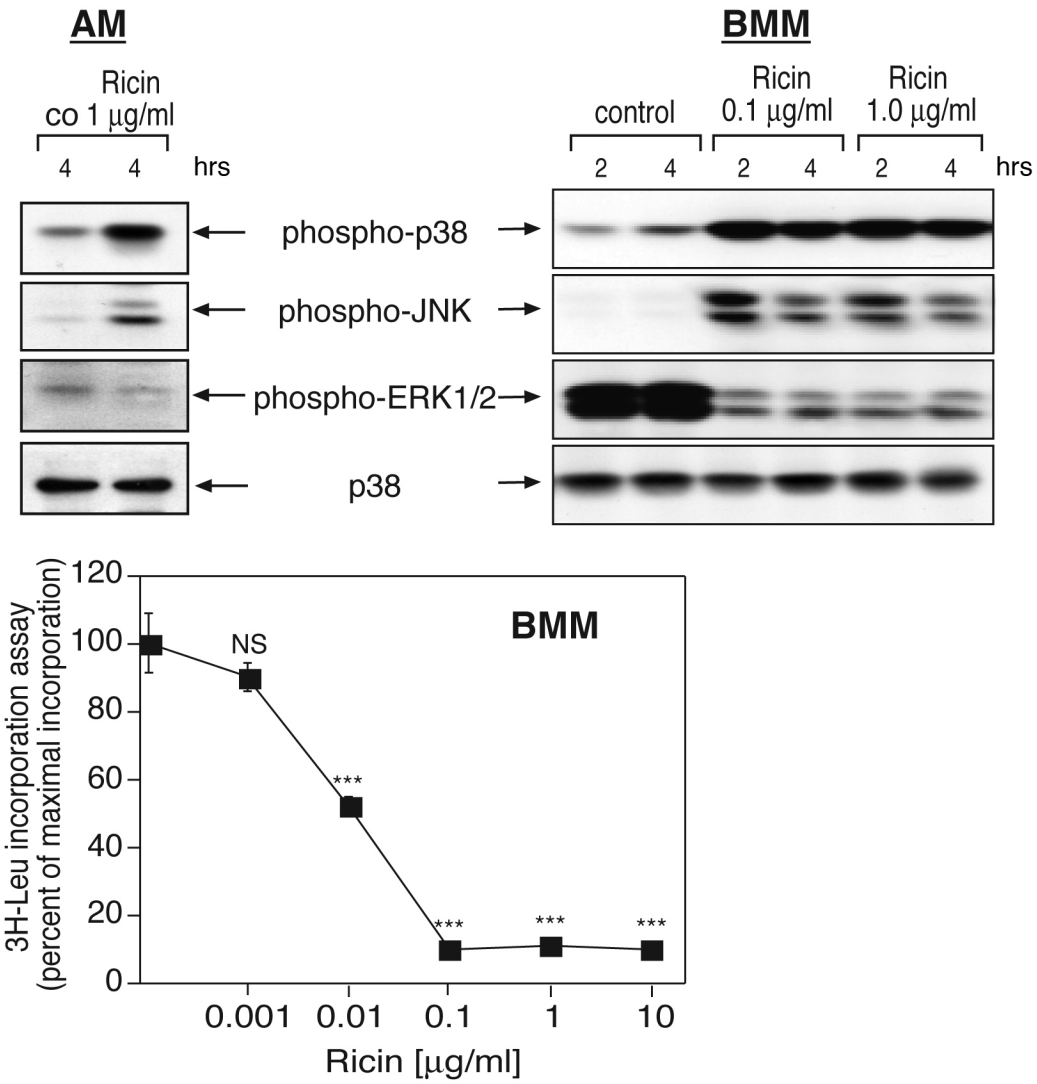


**Figure 2.**

Response of alveolar macrophages (AM) and bone marrow-derived macrophages (BMM) to ricin. Immunoblot analysis of cell lysates from AM (upper left panel) or BMM (upper right panel) exposed to 100 or 1000 ng/ml ricin for 2 or 4 hrs. Antibodies used were reactive against phospho-p38 MAPK, phospho-JNK, phospho-ERK1/2, and p38 (used as a loading control). Lower panel: Inhibition of protein synthesis in BMM, measured by incorporation of [$^3$H]-leucine 3 hrs after the addition of increasing concentrations of ricin. Each treatment was performed in triplicates. Data are presented as mean ± standard error of the mean. Asterisks show comparison between treatments and controls. NS, *not significantly different*; *, $p<0.05$; **, $p<0.01$; ***, $p<0.001$;

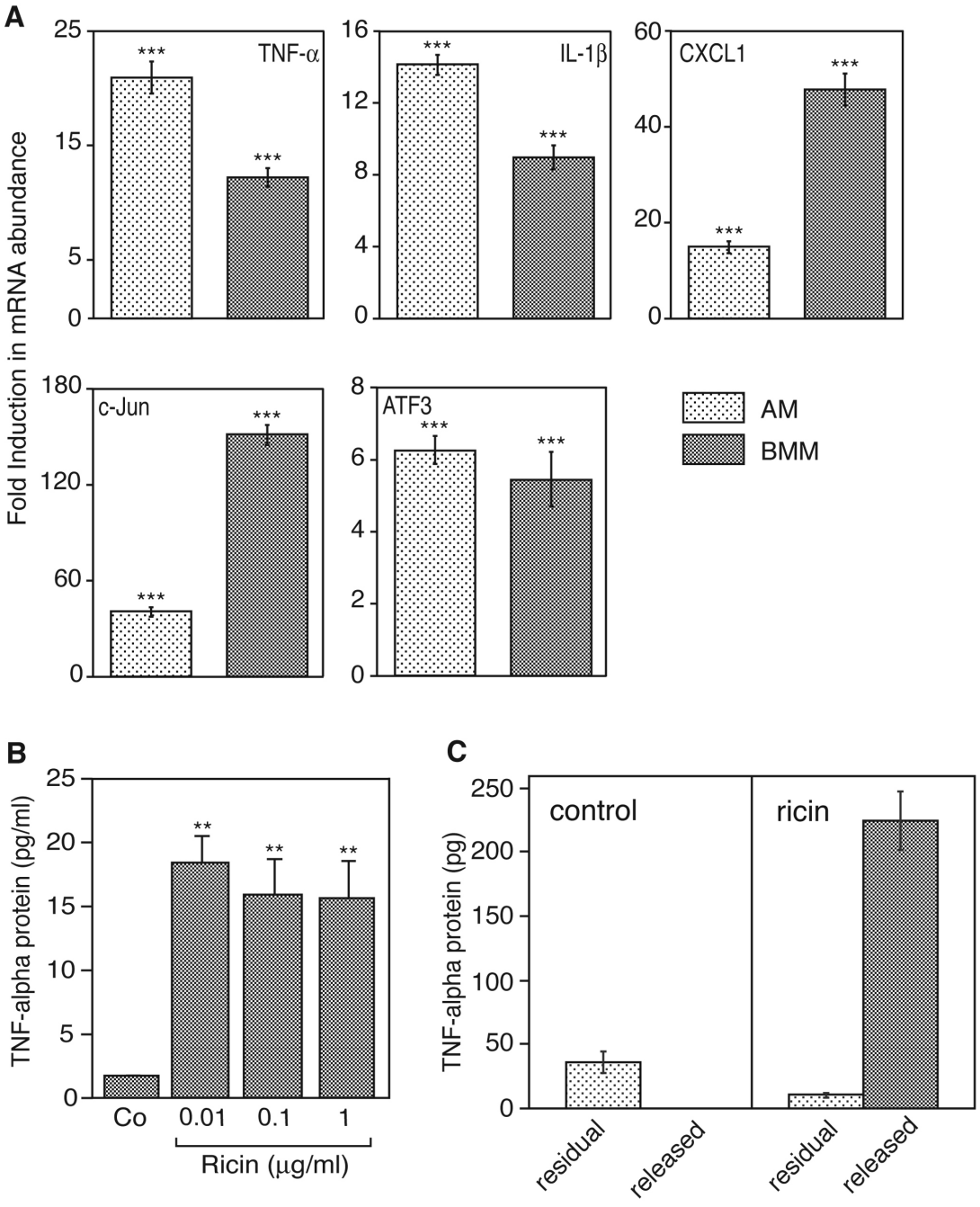


**Figure 3.**

A: Real-time RT-PCR of ricin-induced gene expression in AM and BMM. Cells were exposed to 100 ng/ml ricin for 5 hrs. After RNA extraction, real-time RTPCR was performed, using primers for the corresponding genes. The results were expressed as fold induction, using glyceraldehyde phosphate dehydrogenase (GAPDH) as invariant comparator. Each treatment was performed in triplicate. The experiment was repeated three times, with similar results. Data are displayed as mean ± standard error of the mean. Asterisks above bars show comparison between treatments and controls. ***, p<0.001. *P* values displayed below bars of BMM represent comparison between AM and BMM. NS, *not significantly different;* *, p<0.05; **, p<0.01; ***, p<0.001. B and C: Ricin-induced release of TNF-α protein into the culture

medium of BMM was measured by ELISA. Media were harvested 6 hrs after the addition of ricin. Each treatment was performed on triplicate culture dishes. B: Concentrations of ricin from 10 to 1000 ng/ml were added to macrophage cultures. Data are displayed as mean ± standard error of the mean. Asterisks above bars show comparison between treatments and controls. **, $p<0.01$. C: Cultures of BMM were exposed to diluent control (left panel) or 10 ng/ml ricin (right panel) for 6 hrs, at which time TNF-α protein was measured in the medium (released) and in the cell lysates (residual). Data are displayed as mean ± standard error of the mean. $p<0.01$ for the total TNF-α protein (residual plus released) in control vs. ricin-treated cells.

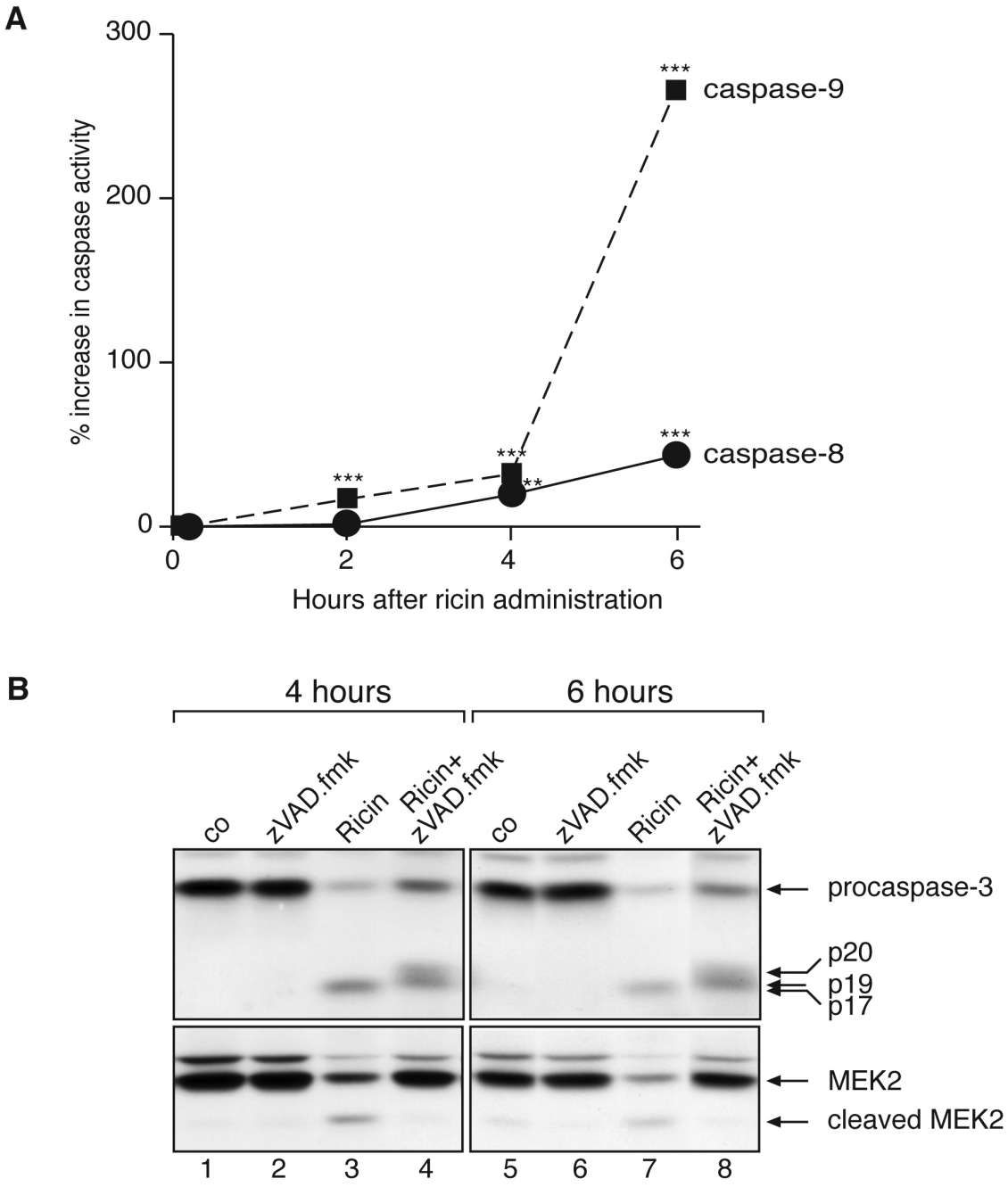


**Figure 4.**

A: Time course of 100 ng/ml ricin on caspase-8 and caspase-9 activity in BMM, measured by using fluorogenic substrates of caspase-8 and -9. Each treatment was performed in triplicate. Values are displayed as mean ± standard error of the mean. Asterisks above bars show comparison between treatments and controls. NS, *not significantly different*; *, $p<0.05$; **, $p<0.01$; ***, $p<0.001$. B: Immunoblot against caspase-3 and MEK2 in BMM after the addition of 100 ng/ml ricin in the presence or absence of a 30 min pretreatment with 25 μM zVAD.fmk.

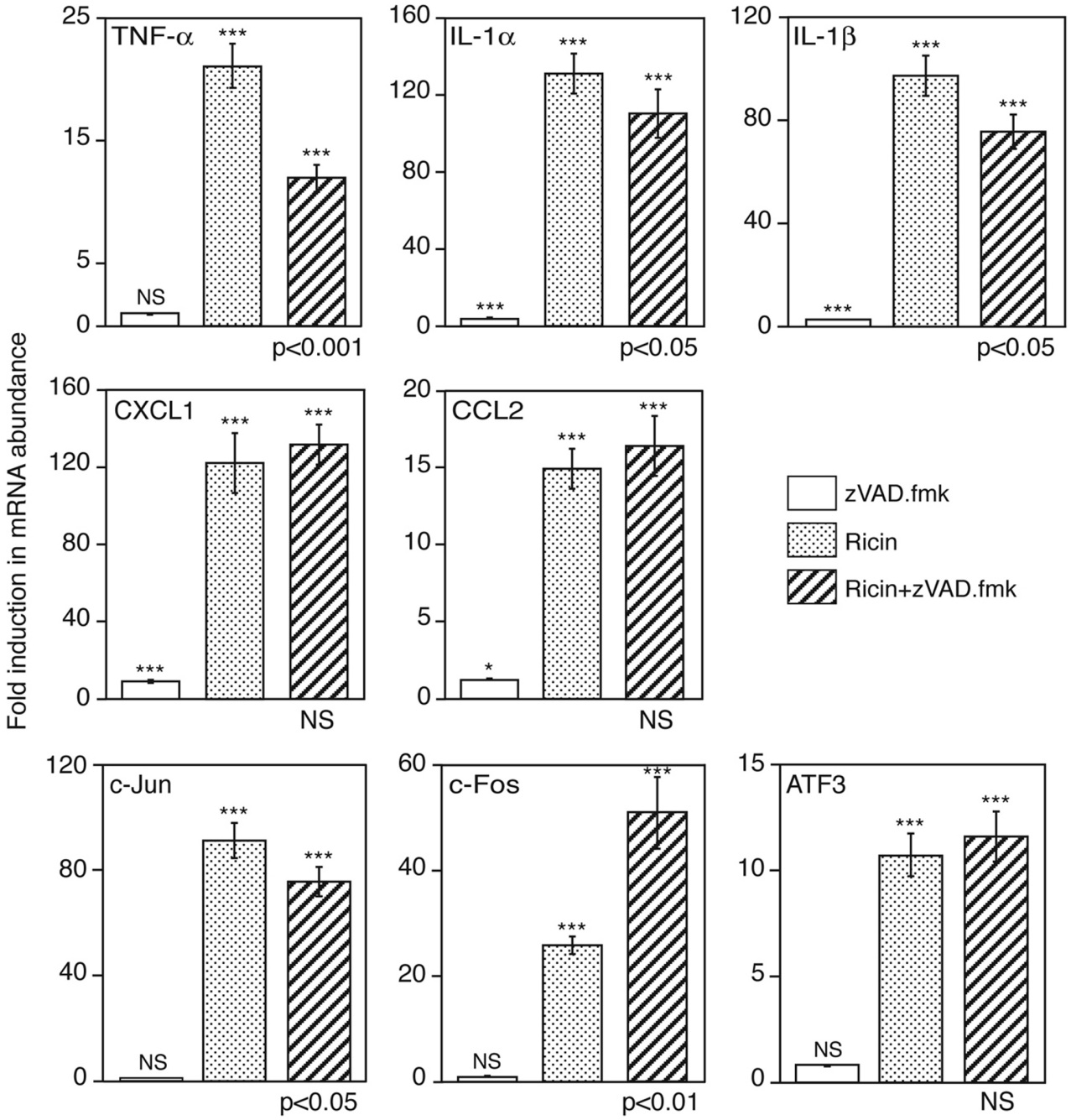


**Figure 5.**

Real-time RT-PCR analysis in BMM after the addition of 100 ng/ml ricin for 5 hrs, in the presence or absence of a 30 min pretreatment with 25 μM zVAD.fmk. The results were expressed as fold induction, using glyceraldehyde phosphate dehydrogenase (GAPDH) as invariant comparator. The experiment was repeated three times, with similar results. Each treatment was performed on triplicate culture dishes. Data are displayed as mean ± standard error of the mean. Asterisks above bars show comparison between treatments and controls; *P* values displayed below bars of ricin plus zVAD.fmk treatment show the comparison of this treatment to treatment by ricin alone. NS, *not significantly different;* *, p<0.05; **, p<0.01; ***, p<0.001.

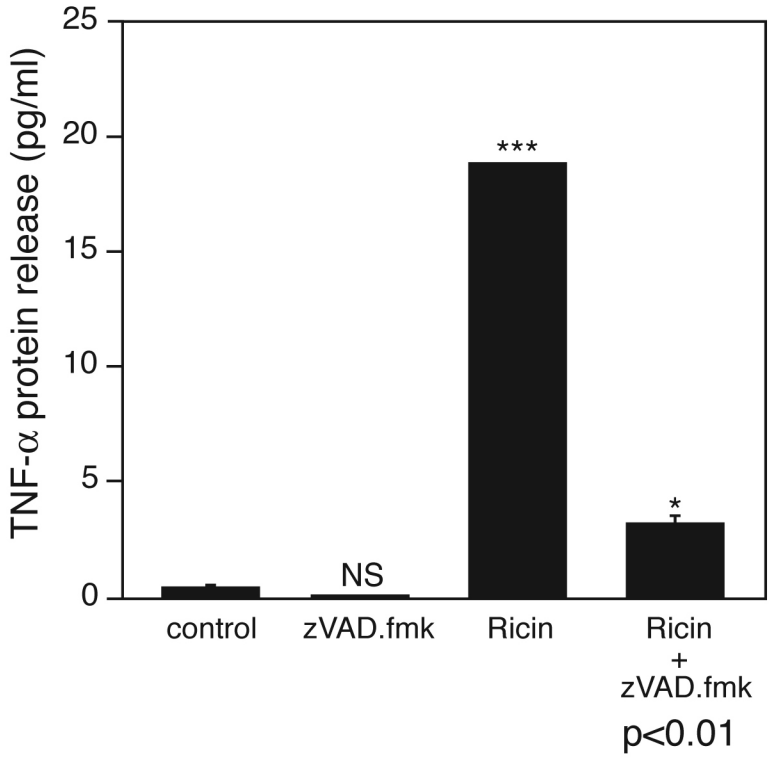


**Figure 6.**

TNF-α protein released into the culture medium after the addition of 100 ng/ml ricin for 6 hrs, in the presence or absence of a 30 min pretreatment with 25 μM zVAD.fmk. Each treatment was performed on triplicate culture dishes. Asterisks above bars show comparison between treatment and control; *P* value displayed below bar of ricin plus zVAD.fmk treatment show the comparison of this treatment to treatment by ricin alone. NS, *not significantly different*; *, p<0.05; **, p<0.01; ***, p<0.001.